

Spin canting due to structural disorder in maghemite

This article has been downloaded from IOPscience. Please scroll down to see the full text article.

1997 J. Phys.: Condens. Matter 9 5461

(<http://iopscience.iop.org/0953-8984/9/25/013>)

View [the table of contents for this issue](#), or go to the [journal homepage](#) for more

Download details:

IP Address: 171.66.16.207

The article was downloaded on 14/05/2010 at 09:01

Please note that [terms and conditions apply](#).

Spin canting due to structural disorder in maghemite

M P Morales†, C J Serna‡, F Bødker§ and S Mørup§

† SEECs, University of Wales, Bangor LL57 1TU, Gwynedd, UK

‡ Instituto de Ciencia de Materiales, CSIC, Cantoblanco 28049 Madrid, Spain

§ Department of Physics, B. 307, Technical University of Denmark, DK-2800 Lyngby, Denmark

Received 4 October 1996, in final form 7 March 1997

Abstract. The spin-canting effect has been studied in samples of maghemite particles with the same width of about 100 nm, but different length and with different degree of cation disorder. Mössbauer spectra obtained at 5 K with a magnetic field of 4 T applied parallel to the propagation direction of the gamma rays showed that there is a correlation between the degree of structural disorder and the spin-canting effect. The results show that the observed spin canting is not a surface effect, but that atoms in the interior of the particles can be significantly influenced by canting effects.

1. Introduction

Ultrafine magnetic particles have important technological applications in, for example, magnetic recording media, ferrofluids and catalysts [1]. It has recently been suggested that such particles can be used for magnetic refrigeration well above liquid helium temperature [2].

The magnetic properties of ultrafine particles depend considerably on the particle size. Particles with dimensions below about 10 nm are often superparamagnetic, i.e. the magnetization vector fluctuates among the easy directions of magnetization [3]. Strong interactions between such small particles may result in ordering of the magnetic moments at low temperatures [4].

Surface effects also have a strong influence on the magnetic properties of small particles. For example, the net magnetization decreases faster with increasing temperature than that of the corresponding bulk materials because a large fraction of the atoms are near the surface where the exchange field is reduced [5]. The magnetic anisotropy energy constant has been found to increase with decreasing particle size, presumably because of the influence of surface anisotropy [6]. Modifications of the surface by chemical treatments have been found to have a strong influence on the coercivity of both metallic [7] and oxide [8] particles.

Maghemite ($\gamma\text{-Fe}_2\text{O}_3$) is ferrimagnetic and small particles of this material are widely used in magnetic recording media and ferrofluids. Therefore the properties of maghemite particles are of great interest. Magnetization measurements [9, 10] have shown that the saturation magnetization decreases with decreasing particle size and this phenomenon has been studied extensively.

^{57}Fe Mössbauer spectroscopy offers a unique possibility to study the approach to magnetic saturation of iron-containing materials. The relative intensities of lines 2 and 5 in the magnetically split six-line spectra depend on the angle between the magnetic hyperfine field and the gamma ray direction. Thus by applying an external magnetic field parallel to

the direction of propagation of the gamma rays one can study the degree of alignment of the spins along the field direction. The ratio of the areas of lines 2 and 5, $I_{2,5}$, and the lines 1 and 6, $I_{1,6}$, is given by [11].

$$I_{2,5}/I_{1,6} = \frac{4 \sin^2 \theta}{3(1 + \cos^2 \theta)} \quad (1)$$

where θ is the angle between the magnetic hyperfine field and the gamma ray direction. Thus for a ferro- or ferrimagnetic material the area of lines 2 and 5 vanishes when the spins are completely aligned with the external field.

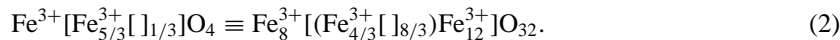
In a study of 6 nm maghemite particles exposed to a magnetic field of 5 T parallel to the gamma ray direction Coey [12] found that the intensity of lines 2 and 5 did not vanish. He suggested that the incomplete alignment of the spins could be explained by the presence of a surface layer with a non-collinear spin structure. Subsequent studies [11] of particles with different size and with and without surface enrichment with ^{57}Fe supported this interpretation. However, this explanation has later been questioned [13, 14].

Parkhurst and Pollard [13] suggested that for Co-doped $\gamma\text{-Fe}_2\text{O}_3$ particles the lack of complete alignment of the spins in large applied fields might be explained by a large magnetic anisotropy energy constant. The doping with Co may indeed increase the magnetic anisotropy energy constant, K , but at least for pure $\gamma\text{-Fe}_2\text{O}_3$ the value of K , which is necessary in order to account for the incomplete alignment of the spins is much larger than the expected value for a magnetic material containing S-state Fe(III) ions in nearly cubic symmetry [15]. Hendriksen *et al* [16] measured the spin alignment in samples of maghemite particles with a preferred orientation of the easy directions of magnetization. These authors found that the degree of canting did not depend on the angle between the applied field and the direction of magnetic texture for applied fields larger than 1 T. These results show that the lack of complete spin alignment in large applied fields cannot be explained by a large magnetic anisotropy [16].

Recently, Parker *et al* [14] found that the degree of canting was identical in maghemite particles with and without a ^{57}Fe enriched surface layer. This result, which contradicts those of earlier studies, suggests that the spin canting is not a surface effect, but that it may be a finite size effect [14]. Thus, although the spin-canting effect in maghemite has been studied for more than 20 years it is still the subject of many investigations and a number of different interpretations have been suggested.

2. Results and discussion

Maghemite possesses the same inverse spinel structure as magnetite (Fe_3O_4) but with some cation vacancies in octahedral positions. As a result, its formula can be written:



The ordering of these vacancies within the octahedral positions can give rise to several crystal symmetries for $\gamma\text{-Fe}_2\text{O}_3$ as indicated by differences in x-ray diffraction patterns. It has been suggested that the vacancies can be distributed: (1) at random (space group $Fd\bar{3}m$); (2) as the lithium cation in $\text{LiFe}_5\text{O}_8 \equiv \text{Fe}_8[\text{Li}_4\text{Fe}_{12}]\text{O}_{32}$ (space group $P4_132$); and (3) with an ordered distribution with tetragonal symmetry (space group $P4_32_12$) [17].

Ideally maghemite is ferrimagnetically ordered with the magnetic moments of the Fe(III) ions in tetrahedral A sites oriented antiparallel to the moments of Fe(III) in the octahedral B sites. The eight filled A sites in the unit cell have moments of $\mu_a = 4.18\mu_B$ and the $13\frac{1}{3}$ filled B sites have moments of $\mu_b = 4.41\mu_B$ [18].

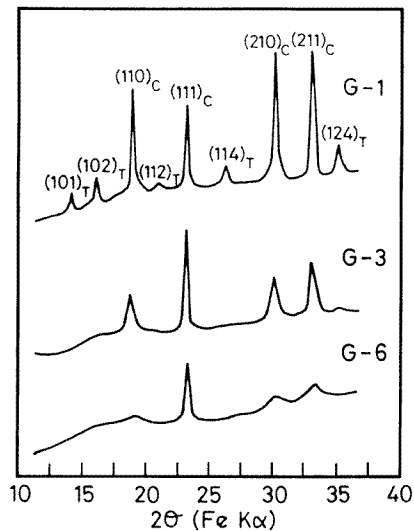


Figure 1. X-ray diffractograms of the three maghemite samples.

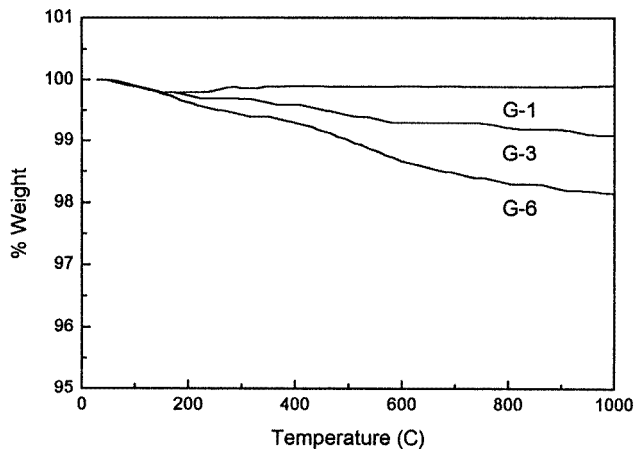


Figure 2. Weight loss as a function of temperature for the three samples.

Recently a new preparation technique, which leads to formation of uniform particles of $\gamma\text{-Fe}_2\text{O}_3$, has been developed [17]. The particles are single crystals as evidenced by x-ray diffraction and high-resolution electron microscopy. In addition, they do not have porosity as manifested by nitrogen absorption isotherms. The specific surface areas were in all cases lower than $10\text{ m}^2\text{ g}^{-1}$. By varying the preparation conditions it is possible to produce particles with different structural disorder.

Figure 1 shows the x-ray diffractograms of three samples with different structural disorder. It should be mentioned that the lattice parameters were identical in the three samples within experimental errors ($a = 8.33 \pm 0.01\text{ \AA}$). Sample G1 clearly shows superlattice reflections ((101), (102), (112), (114), (124)) that can be assigned to a tetragonal cell with $a = 8.33\text{ \AA}$ and $c/a = 3$, according to the space group $P4_32_12$. However, these

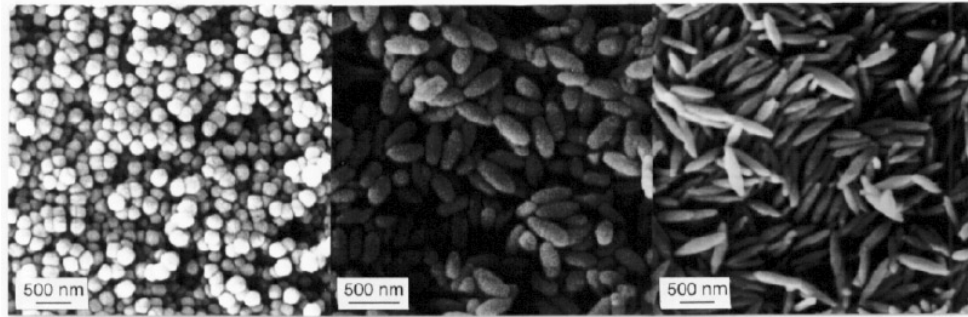


Figure 3. Scanning electron micrographs of the three samples.

reflections do almost but not completely vanish for samples G3 and G6. They have become broadened indicating that the size of the vacancy ordered domains has decreased. Because of the low intensity of these reflections, it is not possible to obtain a reliable estimation of the domain size from the line widths, but the domain size is at least smaller than 5 nm.

Thermogravimetric analysis of the samples (figure 2), shows the weight loss during heating of the γ -Fe₂O₃ particles. At temperatures higher than 360 °C (the temperature at which the transformation from α -Fe₂O₃ to γ -Fe₂O₃ was carried out), the weight loss, probably associated to OH⁻ groups, is negligible for sample G1, 0.4% for G3 and 1.2% for G6. Thus, some chemical defects are still present in the γ -Fe₂O₃ particles, probably located at the boundaries between the ordered domains. The measured weight loss as H₂O corresponds to 0, 1.1 and 3.3 H⁺ ions per tetragonal unit cell in samples G1, G3 and G6, respectively. Before the heat treatment the H⁺ ions may be considered bound to oxygen ions in the close-packed lattice such that the requirement of charge neutrality results in an extra cation vacancy for every three H⁺ ions.

Figure 3 shows scanning electron micrographs of the samples G1, G3 and G6. It can be seen that the particle width differs slightly for the three samples. The particle shape is nearly spherical for sample G1, but is more elongated for the two other samples. The space groups, particle size, obtained from TEM, and saturation magnetization [19] of the three samples are given in table 1.

Table 1. Characteristics of γ -Fe₂O₃ particles. The space group has been assigned considering only the most intense peaks in the x-ray diffractograms although it will be more accurate to consider all the samples belonging to the space group $P4_32_12$ but with a domain size decreasing from sample G1 to G3 and G6.

Sample	Space group	Axial ratio (length/width)	Particle size (nm) TEM	Saturation magnetization (kA m ⁻¹)
G1	$P4_32_12$	1.0 ± 0.1	120 ± 10	352 ± 1
G3	$P4_132$	3.0 ± 0.2	295 ± 20 98 ± 10	340 ± 1
G6	$Fd\bar{3}m$	6.3 ± 0.4	530 ± 25 84 ± 10	309 ± 1

In order to study the influence of cation disorder on the degree of spin canting we have performed Mössbauer studies on these three samples with nearly the same particle width but with different cation disorder.

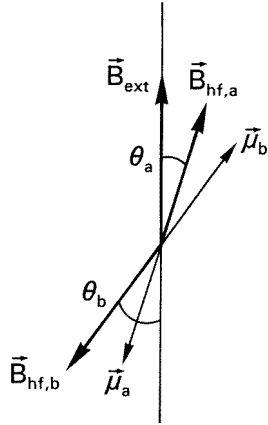


Figure 4. A schematic illustration of the definition of the canting angles θ_a and θ_b .

In Mössbauer spectra of maghemite in zero applied magnetic field the small difference between the hyperfine fields of the iron atoms in the two sublattices results in a partial overlap of the two subspectra due to iron atoms in the A and B sites. For the samples measured here we found a hyperfine field, B_{hf} , of 51.0 ± 0.5 T for the A site and 52.6 ± 0.3 T for the B site at 80 K. In the presence of an external magnetic field, B_{ext} , the effective particle moment is to some degree aligned parallel to the field and the resulting magnetic field at the iron nucleus, B_{obs} , is either enhanced or decreased by the applied field:

$$B_{obs} = B_{hf} \pm B_{ext} \cos \theta \quad (3)$$

where θ is the angle between B_{hf} and B_{ext} (see figure 4).

Figure 5 shows Mössbauer spectra of the three samples at 5 K with a magnetic field of 4.0 T applied parallel to the gamma ray direction.

The spectra were fitted with sextets with the relative areas of the six lines constrained to be $3:X:1:1:X:3$, where the polarization factor $X = 3I_{2,5}/I_{1,6}$ is related to the canting angle θ according to expression (1). In all fits the canting angles for the A and B site magnetic moments, θ_a and θ_b , were considered as two independent parameters.

Different types of other constraints were used in the fits. In one fit it was assumed that both the A and B components consisted of a perfectly aligned component ($X = 0$) and a canted component ($X > 0$). This corresponds to a model in which it is assumed that, for example, the surface spins are canted and the spins in the interior of the particles have a perfect ferrimagnetic structure. Relation (3) was used as an additional constraint in these fits. These constraints resulted in relatively poor fits. In another fitting model it was assumed that all A spins and all B spins have the same canting angle and relation (3) was used as an additional constraint. This model gave significantly better fits (the full curves in figure 5) with the parameters given in table 2. Thus, the analysis of the Mössbauer data indicate that the spin canting is not restricted to a small fraction of the Fe^{3+} ions with a large canting angle and located at the surface and/or at defects. The results rather suggest that most of the Fe^{3+} ions are affected by spin canting with small canting angles. The spin canting may arise from the boundaries between the domains with tetragonal structure and/or from more or less randomly distributed defects associated with OH^- in the structure.

In both types of fits the area ratio of the A and B components were first considered as a free parameter and in later fits constrained to 0.6 in accordance with the assumption

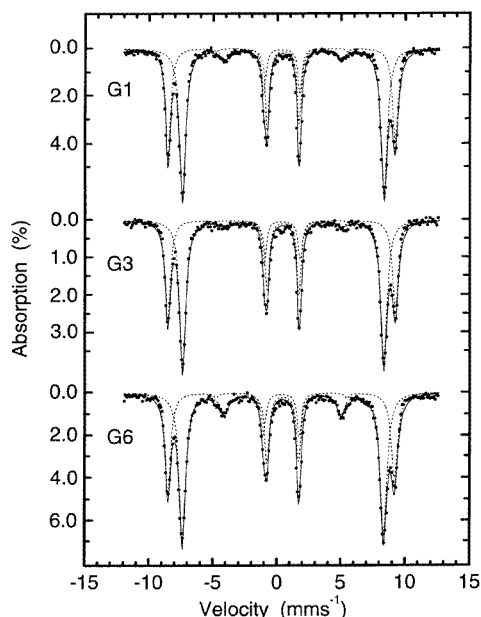


Figure 5. Mössbauer spectra of the three maghemite samples. The spectra were obtained at 5 K with a magnetic field of 4 T applied parallel to the propagation direction of the gamma rays. The best fit with two sextets A and B (shown with the broken curves), constrained as described in the text, is shown by the full curves.

Table 2. Mössbauer parameters obtained from fits of the spectra shown in figure 3 and magnetic moments for the three γ -Fe₂O₃ samples.

Sample	B_{hf} (T)	X	θ	$\mu_{eff}(\mu_B)$	μ_{eff}/μ_{eff-G1}
G1(A)	55.1 ± 0.2	0.07 ± 0.04	10.5 ± 3	22.9 ± 1.3	1.00 ± 0.04
G1(B)	49.1 ± 0.2	0.21 ± 0.06	18.5 ± 3		
G3(A)	55.3 ± 0.2	0.06 ± 0.05	9.6 ± 5	23.9 ± 1.0	1.04 ± 0.04
G3(B)	49.0 ± 0.2	0.14 ± 0.04	15.1 ± 2		
G6(A)	55.0 ± 0.2	0.12 ± 0.07	13.7 ± 4	20.2 ± 1.0	0.88 ± 0.04
G6(B)	48.9 ± 0.2	0.44 ± 0.05	26.4 ± 2		

that all vacancies are in the B sites. This additional constraint did not influence the quality of the fits, indicating that within the experimental uncertainty the Debye–Waller factors of iron atoms in the A and B sites are identical and the vacancy distribution is in accordance with formula (2).

The results given in table 2 show that the canting angle is considerably larger in sample G6 which has most cation disorder while samples G1 and G3 have much lower canting angles. From the canting angles the effective moment per unit cell can be calculated as

$$\mu_{eff} = -N_a\mu_a \cos\theta_a + N_b\mu_b \cos\theta_b \quad (4)$$

where the number of ions on the A site is $N_a = 8$ and the number on the B site is $N_b = 13\frac{1}{3}$. The calculated moments are given in table 2. The results show that the moment for the G6 sample has decreased by about 12% relative to the moment of sample G1 which we

can attribute to the structural disorder. This decrease matches exactly the decrease in the saturation magnetization of sample G6 relative to sample G1 (table 1).

The present results show that the average canting angle in maghemite varies with the degree of structural disorder. In previous work it was found that if the canting effect is a surface phenomenon the thickness of the canted layer should be of the order of 1 nm [11, 16]. We have calculated the fraction of atoms in such a surface layer to be 4.9, 4.7 and 5.1% for the samples G1, G3 and G6, respectively. Such canted surface layers would result in a polarization factor $X \approx 0.07$, i.e. significantly smaller than the measured values. Thus our results show that spin canting can result from structural disorder in maghemite, and that it is not necessarily related to the particle size.

Acknowledgments

This work has been supported by the Danish Council for Natural Sciences and by the Spanish CICYT under project PB95-0002 and CAMST with a short term exchange.

References

- [1] See, for example, Dormann J L and Fiorani D (eds) 1992 *Magnetic Properties of Fine Particles* (Amsterdam: North-Holland)
- [2] McMichael R D *et al* 1992 *J. Magn. Magn. Mater.* **111** 29
Bennett L H *et al* 1993 *J. Appl. Phys.* **73** 6507
Shull R D *et al* 1992 *Magnetic Properties of Fine Particles* ed J L Dormann and D Fiorani (Amsterdam: North-Holland) p 161
- [3] Néel L 1949 *Ann. Geophys.* **5** 99
- [4] Mørup S 1994 *Europhys. Lett.* **28** 671
Mørup S, Bødker F, Hendriksen P V and Linderoth S 1995 *Phys. Rev. B* **52** 287
- [5] Hendriksen P V, Linderoth S and Lindgård P-A 1993 *Phys. Rev. B* **48** 7259
- [6] Bødker F, Mørup S and Linderoth S 1994 *Phys. Rev. Lett.* **72** 282
- [7] Gangopadhyay S *et al* 1992 *Phys. Rev. B* **45** 9778
- [8] Spada F E, Parker F T, Nakakura C Y and Berkowitz A E 1993 *J. Magn. Magn. Mater.* **120** 129
Spada F E, Parker F T, Berkowitz A E and Cox T J 1994 *J. Appl. Phys.* **75** 5562
- [9] Berkowitz A E, Schuele W J and Flanders P J 1968 *J. Appl. Phys.* **39** 1261
- [10] Coey J M D 1987 *Can. J. Phys.* **65** 1210
- [11] Morrish A H and Haneda K 1983 *J. Magn. Magn. Mater.* **35** 105
- [12] Coey J M D 1971 *Phys. Rev. Lett.* **27** 1140
- [13] Pankhurst Q A and Pollard P J 1991 *Phys. Rev. Lett.* **67** 248
- [14] Parker F T, Foster M W, Margulies D T and Berkowitz A E 1993 *Phys. Rev. B* **47** 7885
- [15] Coey J M D 1993 *J. Phys.: Condens. Matter* **5** 7297
- [16] Hendriksen P V, Linderoth S, Oxborrow C A and Mørup S 1994 *J. Phys.: Condens. Matter* **6** 3091
Linderoth S, Hendriksen P V, Bødker F, Wells S, Davies K, Charles S W and Mørup S 1994 *J. Appl. Phys.* **75** 6583
- [17] Morales M P, Pecharroman C, Gonzalez Carreño T and Serna C J 1994 *J. Solid State Chem.* **108** 158
- [18] Greaves C 1983 *J. Solid State Chem.* **49** 325
- [19] Morales M P, de Julián C, González J M and Serna C J 1994 *J. Mater. Res.* **9** 135